Hindawi Publishing Corporation
Journal of Nanomaterials
Volume 2015, Article ID 791063, 8 pages
http://dx.doi.org/10.1155/2015/791063

Research Article

The Efficient Apoptotic Induction of Paclitaxel-Loaded Poly(N-vinylpyrrolidone)-block-poly(ε-caprolactone) Nanoparticles in the In Vitro Study of Lung Cancer Cell Lines

Donghui Zheng,[1] Huiping Ye,[2] Can Luo,[3] Huae Xu,[3] and Ling Meng[3]

[1]*Department of Nephrology, Xuzhou Medical College Affiliated Huai'an Hospital and Huai'an Second Hospital, Huai'an 223002, China*
[2]*Department of Otolaryngology Head and Neck Surgery, Guiyang Medical College Affiliated Hospital and The Affiliated Baiyun Hospital of Guiyang Medical College, Guiyang 550002, China*
[3]*Department of Pharmacy, Nanjing Medical University First Affiliated Hospital, Nanjing 210029, China*

Correspondence should be addressed to Huae Xu; xuhuae@njmu.edu.cn and Ling Meng; mengling-ml@163.com

Received 24 January 2015; Revised 12 March 2015; Accepted 16 March 2015

Academic Editor: Zhuhua Zhang

Paclitaxel (Ptx) has been established as one of the most important components of first line chemotherapy regimen in the treatment of lung cancer. However, the poor solubility of Ptx makes it employ Cremophor as a solvent, which greatly limits its application due to the severe adverse effect. Encapsulation of Ptx into nanoparticles substantially increases the solubility of Ptx, therefore eradicating the necessity of Cremophor involvement. Here we report on a simple way of preparing Ptx-loaded nanoparticles formed by amphiphilic poly(N-vinylpyrrolidone)-block-poly(ε-caprolactone) (PVP-*b*-PCL) copolymers. Ptx was incorporated into PVP-*b*-PCL nanoparticles with a high loading efficiency. In vitro release study shows that Ptx was released from the nanoparticles in a sustained manner. The following experiments including cell staining and cytotoxicity tests indicated that Ptx-NPs led to enhanced induction of apoptosis in non-small-cell lung cancer cell lines NCI-1975 and A549, which is achieved by regulating the expression of apoptosis related proteins. Therefore, data from this study offers an effective way of improving the anticancer efficiency of Ptx by a nanodrug delivery system with amphiphilic PVP-*b*-PCL as drug carriers.

1. Introduction

Lung cancer, one of the most common cancers worldwide, accounts for the most cancer related deaths [1]. Chemotherapy remains to be the most effective way to delay tumor growth. It is demonstrated in numerous studies that paclitaxel (Ptx) has extraordinary activities against a series of cancers by inhibiting the depolymerization of the microtubule, which is essential for cell mitosis [2]. However, poor solubility of Ptx and introduction of Cremophor as solvents in Ptx injection (Taxol) often lead to severe toxicity such as hypersensitivity [3, 4]. Moreover, lack of site specificity of Taxol in clinical application contributes to drug-related side effects, such as neurotoxicity, musculoskeletal toxicity, and neutropenia [5]. Therefore, it is necessary to deliver Ptx in a more effective way to overcome the limitation mentioned above.

Amphiphilic copolymers attract more and more attention as a promising drug delivery system for chemotherapy. In recent years, there are plenty of studies demonstrating the effective antitumor efficacy of Ptx-loaded nanoparticles with amphiphilic copolymers poly(caprolactone)-*b*-poly(ethylene glycol) (PCL-*b*-PEG) and PLGA-*b*-PEG as drug carriers [6, 7]. The amphiphilic copolymers can self-assemble into nanoscaled core-shell spherical particles. The hydrophobic part (e.g., poly(caprolactone) (PCL) or PLGA, PLA) can incorporate hydrophobic drugs as the inner core and the hydrophilic part (e.g., poly(ethylene glycol) (PEG)) can form the outer shell. In previous studies, it has been demonstrated

that Ptx-loaded methoxy PEG-*b*-PCL nanoparticles have a satisfied drug loading efficiency and better in vivo pharmacokinetics [8, 9].

Though PEG possesses several advantages as drug carrier such as good biocompatibility, hydrophilicity, and the absence of antigenicity and immunogenicity [10]; it fails to completely avoid uptake by macrophages and still partially activates complement systems, which leads to a shorter circulation time [11]. In previous studies, poly(N-vinylpyrrolidone) (PVP) is used as an alternative option to PEG due to the more effective avoidance of uptake by reticuloendothelial system (RES) and longer circulation time in vivo [12–14].

Recently it has been reported in several studies that PVP is utilized as the hydrophilic part of the amphiphilic copolymers as drug carriers [12, 15]. For example, Garrec et al. reported the preparation and characterization of Ptx-loaded PVP-*b*-PDLLA nanoparticles with a loading efficiency of about 5% [15]. Most importantly, in our previous studies, we synthesized the copolymer of PVP-*b*-PCL and encapsulated several model drugs with PVP-*b*-PCL as drug carriers [14, 16]. Tetrandrine loaded nanoparticles were also constructed with satisfied loading efficiency and were demonstrated to be effective against lung cancer cell lines [16]. In addition, we successfully formed Ptx-loaded PVP-*b*-PCL nanoparticles with a high loading efficiency [14].

In the current study, we utilized PVP-*b*-PCL as drug carriers and constructed Ptx-loaded nanoparticles (Ptx-NPs). The in vitro cytotoxicity of Ptx-NPs was evaluated in two different kinds of lung adenocarcinoma cells. The following apoptosis induction was then studied to further demonstrate the superior efficiency of Ptx-NPs against free Ptx.

2. Materials and Methods

2.1. Materials. N-Vinylpyrrolidone (98%, Acros) was purified by fractional distillation. ε-Caprolactone (ε-CL, Sigma) was dehydrated by CaH_2 at room temperature and distilled under reduced pressure. Paclitaxel (Ptx) was obtained from Meilian Pharm Co., Ltd. (Chongqing, China). Taxol was purchased from Bristol-Myers Squibb (Princeton, NJ, USA). Human non-small-cell lung cancer cell lines NCI1975 and A549 were obtained from the Shanghai Institute of Cell Biology (Shanghai, China). Cell culture material (RPMI 1640, fetal bovine serum, etc.) was obtained from Life Technologies (Carlsbad, CA, USA). All other chemicals were of analytical grade and used without further purification.

2.2. Methods

2.2.1. Characterization of PVP-b-PCL and Formulation of Nanoparticles. PVP-*b*-PCL was synthesized by ring-opening polymerization as described in our previous reports [14]. ^{1}H-NMR analysis of PVP-*b*-PCL was performed on a 400 MHz Varian VXR-Unity NMR spectrometer. Ptx-NPs were prepared by a nanoprecipitation method as described previously, with minor modification [16, 17]. Briefly, 30 mg PVP-*b*-PCL copolymers and 6 mg Ptx were dissolved in 2 mL acetone. The obtained organic solution was added dropwise into 20 mL distilled water under gentle stirring and at room temperature. The solution was dialyzed in a dialysis bag (molecular weight cutoff 12 kd) to remove acetone thoroughly. The resulting bluish aqueous solution was filtered through a 0.22 μm filter membrane to remove nonincorporated drugs. Drug-free nanoparticles were produced in a similar manner without adding Ptx. Solutions of drug-loaded nanoparticles and empty nanoparticles were then lyophilized with F-68 as cryoprotectants for further utilization.

2.2.2. Characterization of Nanoparticles and Stability Test. Mean diameter and size distribution were measured before lyophilization by photon correlation spectroscopy (dynamic light scattering (DLS)) using a Brookhaven BI-9000 AT instrument (Brookhaven Instruments Corporation, Holtsville, NY, USA). Zeta potential was measured by the laser Doppler anemometry (Zeta Plus, Zeta Potential Analyzer; Brookhaven Instruments Corporation, Holtsville, NY, USA).

The solution of Ptx-NPs was stored at room temperature. Particle sizes were measured by DLS every 2 days for 15 days to evaluate stability.

2.2.3. Drug Loading Content (DLC) and Encapsulation Efficiency (EE). The concentration of Ptx was assayed on a Shimadzu LC-10AD (Shimadzu, Japan) HPLC system equipped with a Shimadzu UV detector and an Agilent C-18, 5 μ, 200 mm × 4.6 mm RP-HPLC analytical column as reported in our previous study [8]. The mobile phase consisted of acetonitrile (spectral grade, Merck, Germany)/double-distilled water (58/42, v/v) pumped at a flow rate of 1.0 mL/min with determination wavelength of 228 nm. The concentration of Ptx was determined based on the peak area at the retention time of 7.3 min by reference to a calibration curve. The following equations were applied to calculate the drug loading content and encapsulation efficiency:

$$\text{Drug loading content (\%)} = \frac{\text{Weight of the drug in nanoparticles}}{\text{Weight of the nanoparticles}} \times 100\%, \quad (1)$$

$$\text{Encapsulation efficiency (\%)} = \frac{\text{Weight of the drug in nanoparticles}}{\text{Weight of the feeding drugs}} \times 100\%. \quad (2)$$

2.2.4. In Vitro Release Study. For in vitro release detection, 5 mg freeze-dried Ptx-NPs were dissolved in 1 mL PBS and then put into a dialysis bag (12 kd cutoff, Sigma), followed by immersion in PBS with slight agitation. At each time point 1 mL samples were taken from the medium outside and quantified for Ptx concentrations by HPLC. After sampling, equal volume of fresh PBS was immediately added into the incubation medium. The concentration of Ptx was expressed as a percentage of the total Ptx in the nanoparticles and plotted as a function of time, respectively.

2.2.5. In Vitro Cytotoxicity Studies. Cytotoxicity of Ptx-NPs against NCI1975 and A549 cells was assessed by MTT assay as reported in our previous study [16]. Briefly, cells were seeded in 96-well plates with a density around 5000 cells/well and allowed to adhere for 24 h prior to the assay. Cells were treated with a series of blank nanoparticles (E-NPs). Cells were exposed to free Ptx and Ptx-NPs at a series of equivalent doses of 10, 20, 40, 80, 160, and 320 ng/mL at 37°C. After 48 h of incubation, cold PBS (pH 7.4) was utilized to wash the cells carefully and then 50 μL of MTT indicator dye (5 mg/mL in PBS, pH 7.4) was added to each well and incubated for 2 h at 37°C in the dark. The medium was withdrawn and 200 μL acidified isopropanol (0.33 mL HCl in 100 mL isopropanol) was added to each well and agitated thoroughly to dissolve the formazan crystals. Absorption was measured at 550 nm in Microkinetics reader BT2000 and obtained values were expressed as a percentage of the controls.

2.2.6. Dual Staining of Cell Apoptosis and Proliferation. NCI1975 cells were treated with 40 μg/mL free Ptx or Ptx-NPs for 48 h and then exposed to 25 mM of 5-ethynyl-29-deoxyuridine (Edu, RiboBio) for 2 h at 37°C followed by the fixation in 4% PFA. After permeabilization with 0.5% Triton-X, the cells were reacted with 16 Apollo reaction cocktail (RiboBio, Guangzhou, China) for 30 min. Subsequently, the DNA contents of the cells were stained with Hoechst 33342 (RiboBio, Guangzhou, China) for 30 min and visualized under a laser scanning confocal microscopy (Leica, TCS Sp5).

2.2.7. Western Blot Analysis. The expression of related proteins was examined by western blot analysis as reported in previous studies [16, 17]. For protein extraction, NCI1975 cells were treated with 40 μg/mL free Ptx or Ptx-NPs for 48 h. Confluent cells were denatured in lysis buffer (20 mM Tris-HCl, 200 mM NaCl, 0.2% Nonidet P-40, 0.5% Triton X-100, and protease inhibitors) and boiled at 95°C for 3 min. Equal amounts of protein extracts were separated on 12% polyacrylamide gels by using standard sodium dodecyl sulfate-polyacrylamide gel electrophoresis (SDS-PAGE) and then transferred onto PVDF membranes (Bio-Rad, Hercules, CA, USA). Following blocking in Tris-buffered saline (TBS) with 0.1% Triton X-100 and 5% milk, the membranes were incubated with different primary antibodies at 4°C overnight. Following washing, the membranes were incubated with secondary antibody conjugated to horseradish peroxidase at room temperature for 2 h. Signal detection was carried out on a G:BOX iChemi imager (Syngene, Frederick, MD, USA) using an enhanced chemiluminescence (ECL) system (Thermo Fisher Scientific Inc., MA, USA).

2.2.8. Caspase-3 Activity Analysis. Cells were cultured under the same conditions as in the western blot analysis. Caspase-3 activity was measured by the caspase colorimetric protease assay kit (Keygen Biotech, Nanjing, China) by following the manufacturer's instruction. The optical density was measured at 405 nm. The obtained values were expressed as folds of controls.

Table 1: Mean particle size and drug load efficiency of Ptx-NPs.

Feeding ratio	Particle size (nm)[a]	Zeta potential (Mv)	DLC (%)[b]	EE (%)[c]
15%	115.5 ± 13.3	−3.2 ± 0.3	17.2 ± 0.5	91.2 ± 2.3

[a]The SD value was for the mean particle size obtained from the three measurements of a single batch.
[b]DLC, drug loading content.
[c]EE, encapsulation efficiency.

2.2.9. Statistical Analysis. The significance of observed differences between groups were analyzed by one-way analysis of variance (ANOVA) followed by taking multiple comparison test using SPSS 11.5 software package (SPSS Inc., IL, USA). Where two groups were compared, independent sample t-tests were applied. Significance was accepted at $P < 0.05$.

3. Results and Discussion

3.1. Characterization of Ptx-NPs

3.1.1. Size, Zeta Potential, and Stability Test. In our previous reports, gel permission chromatography was adopted to detect the molecular weight of PVP-*b*-PCL, which was in accordance with the plan [14]. ^{1}H-NMR analysis (Figure 1(a)) showed that the characteristic peaks in the spectrum were attributed to both PCL and PVP units. In the current study, when the feeding ratio of Ptx was 15%, the mean diameter of Ptx-NPs was about 110 nm with a zeta potential slightly below 0 mV (Table 1 and Figure 1(b)). As reported in a previous study, the PVP outer shell could screen the surface charge to a certain degree, which gives the explanation of the near neutral zeta potential of Ptx-NPs [14, 17]. In addition, the size of Ptx-NPs underwent slight changes during 11 days in routine temperature, which indicates the good stability of Ptx-NPs in vitro (Figure 1(c)).

3.1.2. Drug Loading Content and Encapsulation Efficiency. As shown in Table 1, the highest drug loading content of Ptx-NPs was about 17.2 ± 0.5% and the encapsulation efficiency was more than 90%. It is reported previously that high loading efficiency was mainly due to the high affinity of the loaded hydrophobic drug and the PCL core, which also contributed to the satisfied stability of the drug-loaded nanoparticles [17, 18]. According to the previous studies, Ptx loading efficiency varied from 5% to 25% depending on the different polymers [6, 7]. There are some studies reporting the loading efficiency of Ptx in PVP-*b*-PCL nanoparticles being about 8–25% with different feeding ratios [14].

3.2. In Vitro Release Study. In the in vitro release study, Ptx was released from the nanoparticles in a sustained manner. The initial burst release in the first 5 hours was mainly attributed to the drugs adhering to the surface of nanoparticles. After that, sustained release of Ptx was observed due to the continuous release of encapsulated Ptx from the core of nanoparticles (Figure 1(d)). Therefore, results from the release study showed that the release pattern of Ptx-NPs

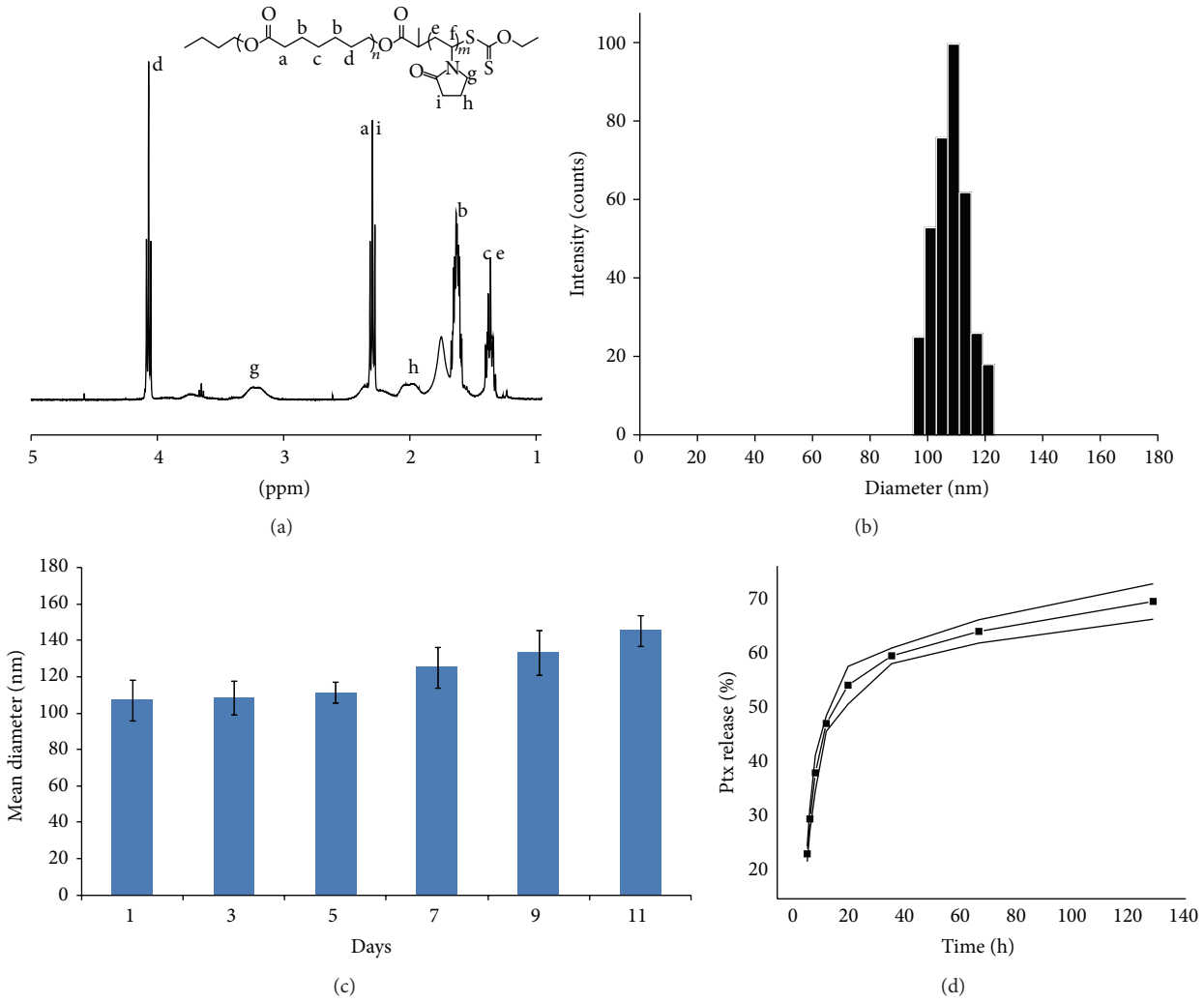

Figure 1: Characterization of PVP-*b*-PCL and Ptx-loaded nanoparticles. (a) ^{1}H-NMR spectrum of PVP-*b*-PCL. (b) Size distribution of Ptx-NPs measured by DLS. (c) Size changes of Ptx-NPs at room temperature. (d) Cumulative release profile of Ptx from PVP-*b*-PCL nanoparticles.

rendered it to be a promising controlled release system of Ptx for cancer therapy.

3.3. In Vitro Cytotoxicity. The viability of NCI 1975 and A549 cells exposed to a series of concentrations of Ptx or Ptx-NPs was detected by MTT assay. Blank nanoparticles were almost nontoxic to two kinds of lung adenocarcinoma cells as shown in Figure 5. The maximum dose of 600 μg/mL led to a less than 10% cell death of two kinds of cells, which means a high dose of PVP-*b*-PCL is of good biocompatibility (Figure 2).

Figure 3 indicated the cytotoxicity of Ptx and Ptx-NPs against two kinds of lung cancer cells. Both NCI1975 and A549 cells underwent a dose-dependent reduction in viability when exposed to a series of escalated doses of Ptx or Ptx-NPs. Most importantly, Ptx-NPs led to more cell death than the equivalent dose of free Ptx. The IC50 values of Ptx and Ptx-NPs against NCI1975 cells were 79.4 and 42.1 ng/mL, respectively. In addition, Ptx-NPs surpassed free Ptx in inhibiting

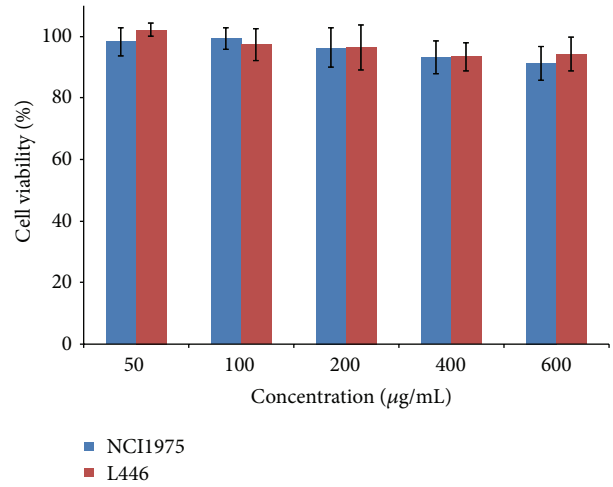

Figure 2: Cytotoxicity of blank PVP-*b*-PCL nanoparticles on NCI1975 and A549 cells.

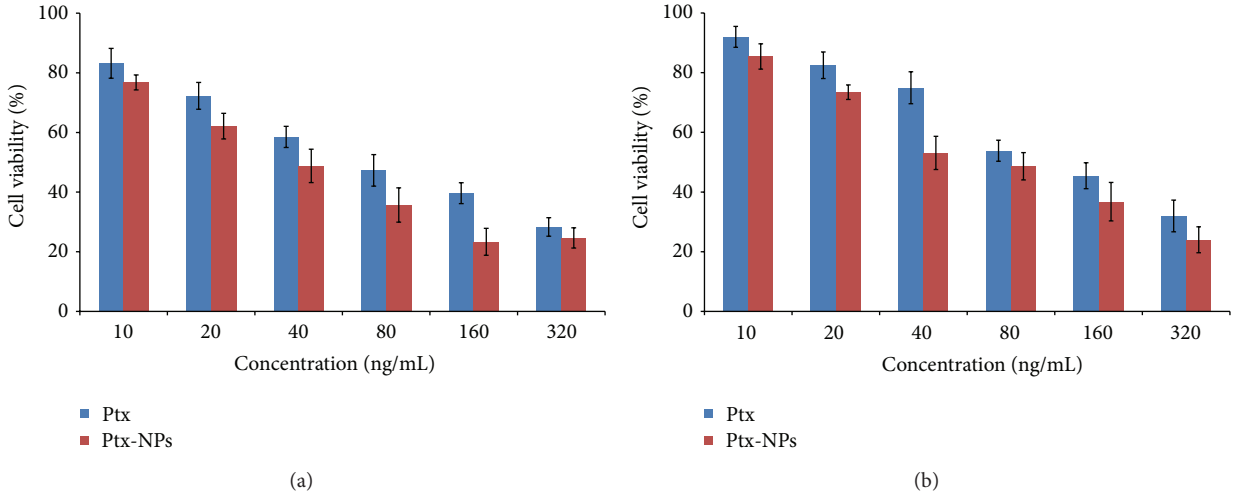

Figure 3: Cytotoxicity of Ptx and Ptx-NPs on NCI1975 and A549 cells. (a) Dose-dependent cytotoxicity of free Ptx and Ptx-NPs against NCI1975 cells. (b) Dose-dependent cytotoxicity of free Ptx and Ptx-NPs against A549 cells. Data are presented as mean ± SD ($n = 3$).

the growth of A549 cells with an IC50 value of 124.4 over 72.1 ng/mL. The results from the in vitro cytotoxicity proved the superior antitumor effect of Ptx-NPs over free Ptx, which was in accordance with the findings in our previous study that drug-loaded nanoparticles could inhibit the growth of tumor cells more effectively through highly efficient cellular uptake than the equivalent dose of free drug [8, 10, 17]. As reported previously, nanoparticle-based cellular uptake was mainly through endocytosis, which was more efficient than the cell membrane penetration of small molecules. Since two kinds of cells were both non-small-cell lung cancer cell lines, the following apoptotic experiments were performed on NCI1975 cells.

3.4. Dual Cell Staining of Apoptosis and Proliferation. To further evaluate the apoptosis-inducing and antiproliferative effect of Ptx-NPs, cells were dual-stained by Hoechst 33342 and Edu. As to Hoechst 33342 staining, live cells have normal blue nucleuses while apoptotic cells appear to have bright blue nucleuses with distinctive condensed or fragmented chromatin. On the contrary, Edu incorporation assay was performed to detect the proliferation of cells exposed to different agents [19, 20]. Figure 4 showed that the cells, exposed to either Ptx or Ptx-NPs, with condensed blue nucleuses stained by Hoechst 33342 were more than those in the control group. In addition, there were less Edu-positive cells in the group treated with Ptx or Ptx-NPs compared with the control group. Most importantly, the number of apoptotic cells in Ptx-NPs group was significantly higher than that in Ptx group, whereas the number of Edu-positive cells in Ptx-NPs groups was significantly lower. Therefore, it is concluded that Ptx-NPs could lead to more cell apoptosis and inhibit cell proliferation more significantly than the equivalent dose of Ptx did.

3.5. Evaluation of Apoptosis through the Expression of Apoptotic Proteins and Caspase-3 Activity. It is reported that apoptosis is characterized by the imbalance of proapoptotic and antiapoptotic proteins, which leads to the activation of caspase castrade [21]. Among the apoptotic proteins, Bcl-2 family, including the antiapoptotic Bcl-2 and proapoptotic Bax proteins, plays an important role in regulating the onset of apoptosis [22, 23]. Elevation of Bax/Bcl-2 ratio results in the initiation of apoptosis. Here we detected the expression of apoptotic proteins in cells treated with the equivalent dose of Ptx and Ptx-NPs. Ptx-NPs treatment increased the expression of Bax and attenuated the expression of Bcl-2, which revealed a significant alteration between the groups receiving Ptx and Ptx-NPs (Figure 5).

The extent of apoptosis could also be evaluated by the activity of caspase-3 [24, 25]. As shown in Figure 6, both Ptx-NPs and Ptx activated caspase-3 more significantly than control. In detail, 40 ng/mL Ptx increased the activity of caspase-3 with about 4-fold while the equivalent dose of Ptx-NPs led to a nearly 7-fold augment.

Results from the current study demonstrated that delivery of Ptx by PVP-*b*-PCL nanoparticles was capable of inhibiting the proliferation and inducing the apoptosis of lung adenocarcinoma cells more efficiently than free Ptx. According to the current and our previous studies, the difference in apoptosis induction between free Ptx and Ptx-NPs may be attributed to the different ways of cell penetration [8, 18]. Compared to the infiltration of small molecules of free Ptx, the cellular uptake of Ptx-NPs mediated by endocytosis leads to more efficient intracellular accumulation of Ptx, which consequently induces more cellular apoptosis by altering the expression of apoptosis related proteins [26, 27].

4. Conclusions

In the current study, we reported a simple and stable way to construct Ptx-loaded PVP-*b*-PCL nanoparticles. The obtained Ptx-NPs were then characterized by their

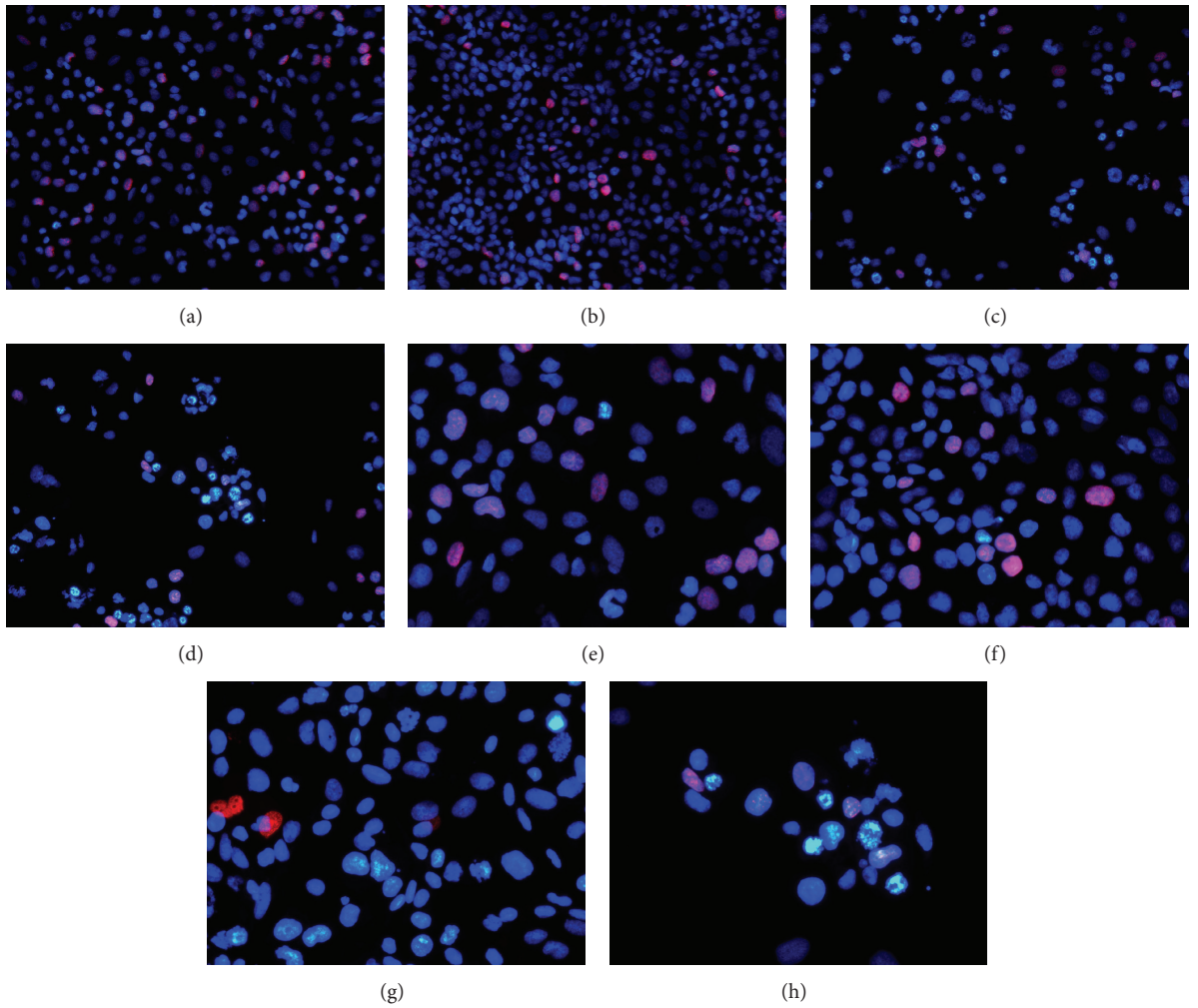

Figure 4: Dual staining of NCI1975 cells by Hoechst 33342 and Edu when treated with the equivalent dose of Ptx and Ptx-NPs. (a), (e) Lower and higher magnification fluorescent field of cells in the control group. (b), (f) Lower and higher magnification fluorescent field of cells treated with blank nanoparticles. (c), (g) Lower and higher magnification fluorescent field of cells treated with free Ptx at a dose of 40 μg/mL. (d), (h) Lower and higher magnification fluorescent field of cells treated with Ptx-NPs at an equivalent dose of 40 μg/mL.

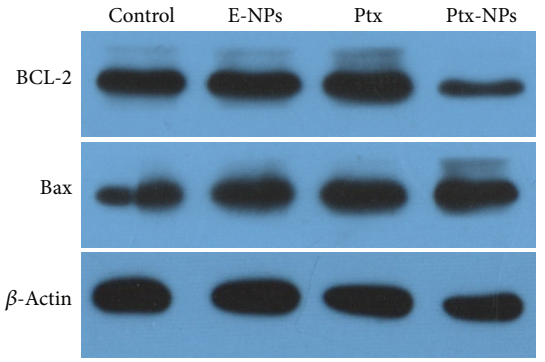

Figure 5: The expression of antiapoptotic protein Bcl-2 and proapoptotic protein Bax in NCI1975 cells exposed to the equivalent dose of Ptx or Ptx-NPs detected by western blot analysis.

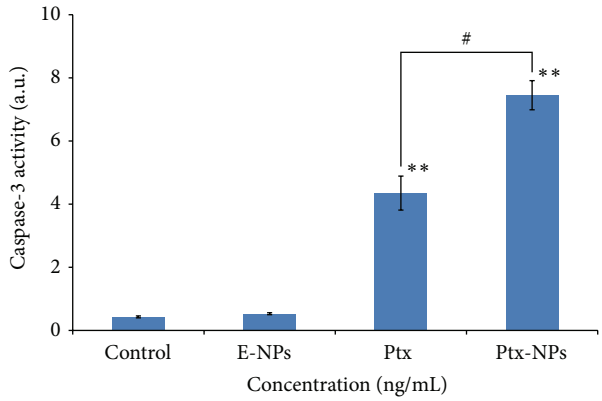

FIGURE 6: Caspase-3 activities in cells treated with an equivalent dose of Ptx or Ptx-NPs. ** represents $P < 0.01$ versus control; # represents $P < 0.05$.

physiochemical properties. Ptx was incorporated into the nanoparticles with a high loading efficiency. In vitro release study revealed that Ptx was released from the nanoparticles in a sustained manner. Cytotoxicity test indicated that Ptx-NPs dose-dependently inhibited the proliferation and induced the apoptosis of tumor cells more effectively by regulating the apoptotic proteins Bcl-2 and Bax. Therefore, data from this study prove the antitumor potential of Ptx by a nanodrug delivery system with amphiphilic PVP-*b*-PCL as drug carriers.

Conflict of Interests

The authors declare no conflict of interests.

Authors' Contribution

Donghui Zheng, Huiping Ye, and Can Luo contributed equally to this work.

Acknowledgments

This work was supported by the National Natural Science Foundation of China (nos. 81101902 and 81270817), A Project Funded by the Priority Academic Program Development of Jiangsu Higher Education Institutions (PAPD), and Guizhou Scientific Grant LG2012-068.

References

[1] R. Siegel, D. Naishadham, and A. Jemal, "Cancer statistics, 2013," *CA—Cancer Journal for Clinicians*, vol. 63, no. 1, pp. 11–30, 2013.

[2] E. J. Woodward and C. Twelves, "Scheduling of taxanes: a review," *Current Clinical Pharmacology*, vol. 5, no. 3, pp. 226–231, 2010.

[3] R. T. Dorr, "Pharmacology and toxicology of Cremophor EL diluent," *Annals of Pharmacotherapy*, vol. 28, no. 5, supplement, pp. S11–S14, 1994.

[4] J. Liebmann, J. A. Cook, and J. B. Mitchell, "Cremophor EL, solvent for paclitaxel, and toxicity," *The Lancet*, vol. 342, no. 8884, p. 1428, 1993.

[5] C. Tate, "Paclitaxel: infusion duration effect on toxicity and efficacy," *Cancer Control*, vol. 2, no. 1, pp. 58–61, 1995.

[6] M. L. Forrest, J. A. Yáñez, C. M. Remsberg, Y. Ohgami, G. S. Kwon, and N. M. Davies, "Paclitaxel prodrugs with sustained release and high solubility in poly(ethylene glycol)-b-poly(ε-caprolactone) micelle nanocarriers: pharmacokinetic disposition, tolerability, and cytotoxicity," *Pharmaceutical Research*, vol. 25, no. 1, pp. 194–206, 2008.

[7] R. Yang, F. Meng, S. Ma, F. Huang, H. Liu, and Z. Zhong, "Galactose-decorated cross-linked biodegradable poly(ethylene glycol)-*b*-poly(ε-caprolactone) block copolymer micelles for enhanced hepatoma-targeting delivery of paclitaxel," *Biomacromolecules*, vol. 12, no. 8, pp. 3047–3055, 2011.

[8] K. Letchford, R. Liggins, K. M. Wasan, and H. Burt, "In vitro human plasma distribution of nanoparticulate paclitaxel is dependent on the physicochemical properties of poly(ethylene glycol)-block-poly(caprolactone) nanoparticles," *European Journal of Pharmaceutics and Biopharmaceutics*, vol. 71, no. 2, pp. 196–206, 2009.

[9] C. Wang, Y. Wang, Y. Wang, M. Fan, F. Luo, and Z. Qian, "Characterization, pharmacokinetics and disposition of novel nanoscale preparations of paclitaxel," *International Journal of Pharmaceutics*, vol. 414, no. 1-2, pp. 251–259, 2011.

[10] Y. Hu, J. Xie, Y. W. Tong, and C.-H. Wang, "Effect of PEG conformation and particle size on the cellular uptake efficiency of nanoparticles with the HepG2 cells," *Journal of Controlled Release*, vol. 118, no. 1, pp. 7–17, 2007.

[11] T. Ishida, M. Ichihara, X. Wang et al., "Injection of PEGylated liposomes in rats elicits PEG-specific IgM, which is responsible for rapid elimination of a second dose of PEGylated liposomes," *Journal of Controlled Release*, vol. 112, no. 1, pp. 15–25, 2006.

[12] A. Leiva, F. H. Quina, E. Araneda, L. Gargallo, and D. Radić, "New three-arm amphiphilic and biodegradable block copolymers composed of poly(ε-caprolactone) and poly(N-vinyl-2-pyrrolidone). Synthesis, characterization and self-assembly in aqueous solution," *Journal of Colloid and Interface Science*, vol. 310, no. 1, pp. 136–143, 2007.

[13] Y. Kaneda, Y. Tsutsumi, Y. Yoshioka et al., "The use of PVP as a polymeric carrier to improve the plasma half-life of drugs," *Biomaterials*, vol. 25, no. 16, pp. 3259–3266, 2004.

[14] Z. Zhu, Y. Li, X. Li et al., "Paclitaxel-loaded poly(*N*-vinylpyrrolidone)-*b*-poly(ε-caprolactone) nanoparticles: preparation and antitumor activity *in vivo*," *Journal of Controlled Release*, vol. 142, no. 3, pp. 438–446, 2010.

[15] D. Le Garrec, S. Gori, L. Luo et al., "Poly(N-vinylpyrrolidone)-block-poly(d,l-lactide) as a new polymeric solubilizer for hydrophobic anticancer drugs: In vitro and in vivo evaluation," *Journal of Controlled Release*, vol. 99, no. 1, pp. 83–101, 2004.

[16] H. Xu, Z. Hou, H. Zhang et al., "An efficient Trojan delivery of tetrandrine by poly(N-vinylpyrrolidone)-block-poly(epsilon-caprolactone) (PVP-b-PCL) nanoparticles shows enhanced apoptotic induction of lung cancer cells and inhibition of its migration and invasion," *International Journal of Nanomedicine*, vol. 9, no. 1, pp. 231–242, 2014.

[17] X. Li, X. Lu, H. Xu et al., "Paclitaxel/tetrandrine coloaded nanoparticles effectively promote the apoptosis of gastric cancer cells based on 'oxidation therapy'," *Molecular Pharmaceutics*, vol. 9, no. 2, pp. 222–229, 2012.

[18] R. Fatemeh, S. Naznin, A. Davood, and N. Farnaz, "Effects of chitosan concentration on the protein release behaviour of electrospun poly(ε-caprolactone)/chitosan nanofibers," *Journal of Nanomaterials*. In press.

[19] D. Qu, G. Wang, Z. Wang et al., "5-Ethynyl-2′-deoxycytidine as a new agent for DNA labeling: detection of proliferating cells," *Analytical Biochemistry*, vol. 417, no. 1, pp. 112–121, 2011.

[20] T. Zeng, H. Gao, P. Yu et al., "Up-regulation of kin17 is essential for proliferation of breast cancer," *PLoS ONE*, vol. 6, no. 9, Article ID e25343, 2011.

[21] G. T. Williams and C. A. Smith, "Molecular regulation of apoptosis: genetic controls on cell death," *Cell*, vol. 74, no. 5, pp. 777–779, 1993.

[22] J. M. Hardwick, Y.-B. Chen, and E. A. Jonas, "Multipolar functions of BCL-2 proteins link energetics to apoptosis," *Trends in Cell Biology*, vol. 22, no. 6, pp. 318–328, 2012.

[23] J. M. Adams and S. Cory, "The Bcl-2 protein family: arbiters of cell survival," *Science*, vol. 281, no. 5381, pp. 1322–1326, 1998.

[24] G. S. T. Smith, J. A. M. Voyer-Grant, and G. Harauz, "Monitoring cleaved caspase-3 activity and apoptosis of immortalized oligodendroglial cells using live-cell imaging and cleaveable fluorogenic-dye substrates following potassium-induced membrane depolarization," *Journal of Visualized Experiments*, no. 59, Article ID e3422, 2012.

[25] B. Canbakan, H. Senturk, M. Canbakan, T. Toptas, and M. Tuncer, "Reliability of caspase activity as a biomarker of hepatic apoptosis in nonalcoholic fatty liver disease," *Biomarkers in Medicine*, vol. 5, no. 6, pp. 813–815, 2011.

[26] M. Yin, Y. Yin, Y. Han, H. Dai, and S. Li, "Effects of uptake of hydroxyapatite nanoparticles into hepatoma cells on cell adhesion and proliferation," *Journal of Nanomaterials*, vol. 2014, Article ID 731897, 7 pages, 2014.

[27] J. Mao, L. Wang, Z. Qian, and M. Tu, "Uptake and cytotoxicity of Ce(IV) doped TiO_2 nanoparticles in human hepatocyte cell line L02," *Journal of Nanomaterials*, vol. 2010, Article ID 910434, 8 pages, 2010.